

HYMACS in ICON

First idealized tests and adaptations of the dynamical core to subgrid-scale mass fluxes

Michael Langguth, Volker Kuell and Andreas Bott



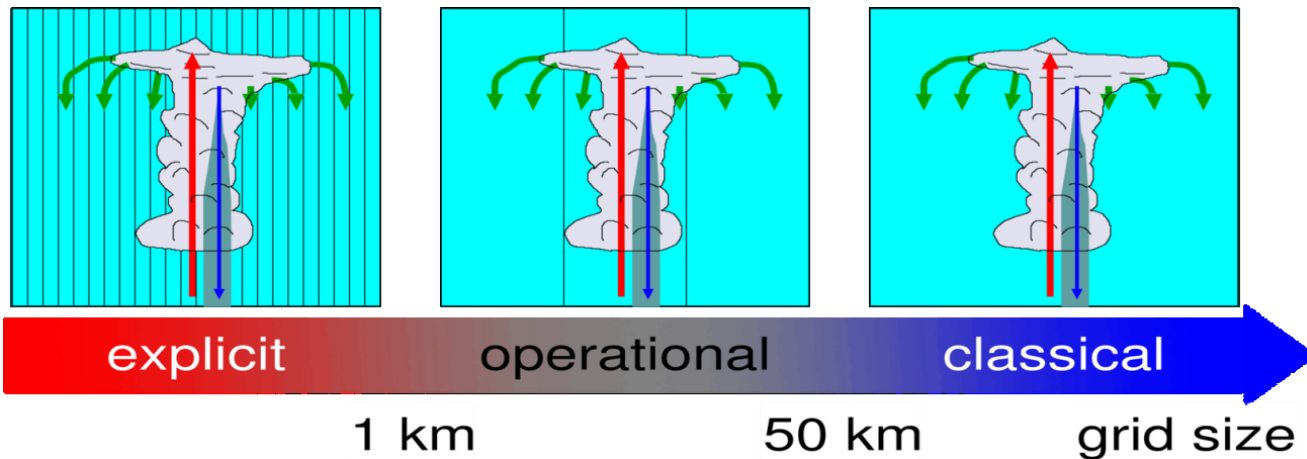
Sturmjäger NRW

ICCARUS 2019
DWD, Offenbach, 18th-20th March 2019

Offenbach, 2019/03/18

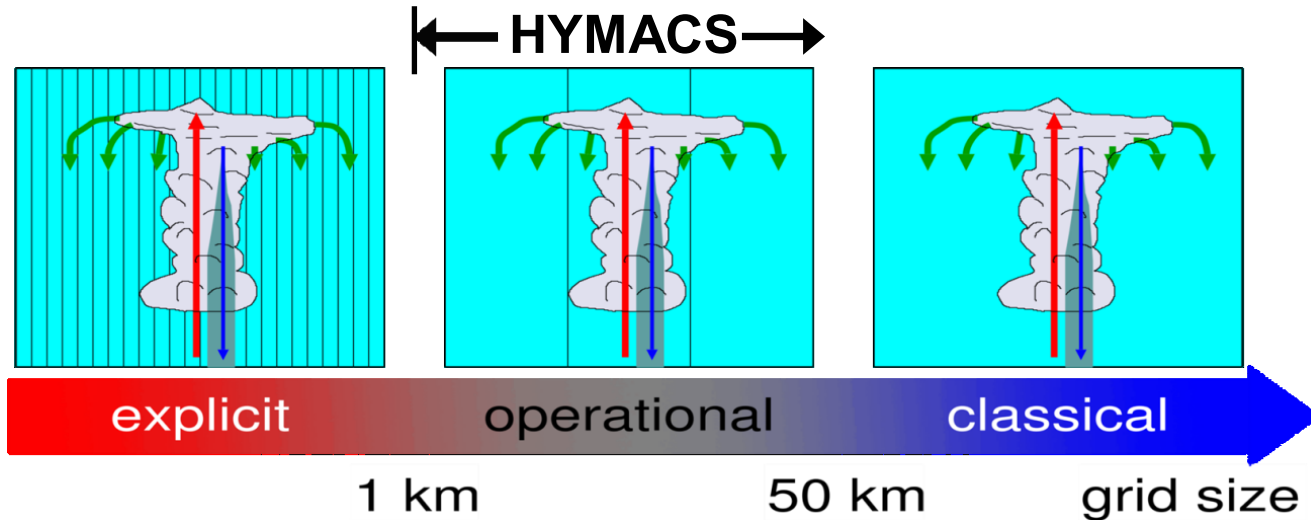
Motivation

- Cumulus convection: major driver for atmospheric dynamics
- NWP models (still) require convection parametrization schemes, but operate in convective grey zone
 - conceptual adaptations required
- **Hybrid Mass Flux Convection Scheme (HYMACS)** abandons assumption of local subsidence → local mass sources / sinks
- Merit of HYMACS in COSMO (*Kuell and Bott, 2009, 2011; Uebel and Bott, 2015* etc.), in WRF (*Ong et al., 2017*)



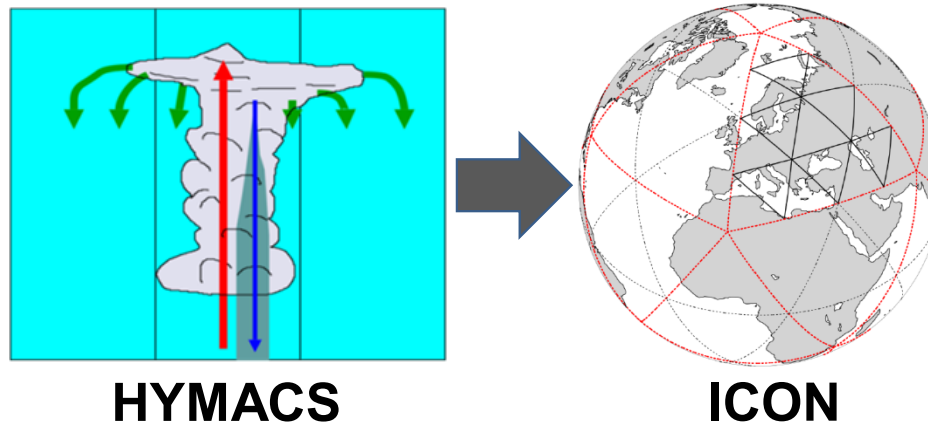
Motivation

- Cumulus convection: major driver for atmospheric dynamics
- NWP models (still) require convection parametrization schemes, but operate in convective grey zone
 - conceptual adaptations required
- **Hybrid Mass Flux Convection Scheme (HYMACS)** abandons assumption of local subsidence → local mass sources / sinks
- Merit of HYMACS in COSMO (*Kuell and Bott, 2009, 2011; Uebel and Bott, 2015* etc.), in WRF (*Ong et al., 2017*)



Motivation

- Cumulus convection: major driver for atmospheric dynamics
- NWP models (still) require convection parametrization schemes, but operate in convective grey zone
 - conceptual adaptations required
- **Hybrid Mass Flux Convection Scheme (HYMACS)** abandons assumption of local subsidence → local mass sources / sinks
- Merit of HYMACS in COSMO (*Kuell and Bott, 2009, 2011; Uebel and Bott, 2015* etc.), in WRF (*Ong et al., 2017*)



HYMACS core

- HYMACS introduces an additional convective mass flux term \mathbf{J}_c in the continuity equation

$$\frac{\partial \rho}{\partial t} = -\nabla \cdot (\rho \mathbf{v}_e) + \left. \frac{\partial \rho}{\partial t} \right|_{\text{conv}} = 0 \quad \text{with} \quad \left. \frac{\partial \rho}{\partial t} \right|_{\text{conv}} = -\nabla \cdot \mathbf{J}_c = -\frac{1}{A_c} \left(\frac{\partial M_u}{\partial z} + \frac{\partial M_d}{\partial z} \right)$$

Local change in density through **grid scale** (calculated in the dynamical core) and **convective** (to be parametrized) mass flux divergence

- Physics-dynamics coupling is neither isobaric nor isochoric!
- Cloud model also gives convective tendencies of enthalpy h , of specific moisture species q^x and horizontal momentum \mathbf{v}_h
- Convective Exner pressure tendency:

$$\left. \frac{\partial \pi}{\partial t} \right|_{\text{conv}} = f \left(\left. \frac{\partial h}{\partial t} \right|_{\text{conv}}, \left. \frac{\partial \rho}{\partial t} \right|_{\text{conv}}, \left. \frac{\partial q^x}{\partial t} \right|_{\text{conv}} \right)$$

Mass Lifting Experiment

Approach

Compare mass lifting experiments in ICON with experiments in COSMO (see *Kuell et al., 2007*)

General Model Setup

Dry, polytrope ($\frac{dT}{dz} = -6 \text{ K/km}$) background atmosphere at rest

69 equidistant vertical levels ($\Delta z = 300 \text{ m}$)

Rayleigh sponge layer @ $z \geq 14 \text{ km}$

Central grid column with mass sink (bottom layer) and mass source (@ $z = 8.85 \text{ km}$) \rightarrow 1 hour „convective cell“

Mass transfer only \rightarrow no enthalpy tendency

Specific COSMO Setup

Rectangular grid with
 $\Delta x_{\text{COS}} = 0.0625^\circ \cong 7 \text{ km}$

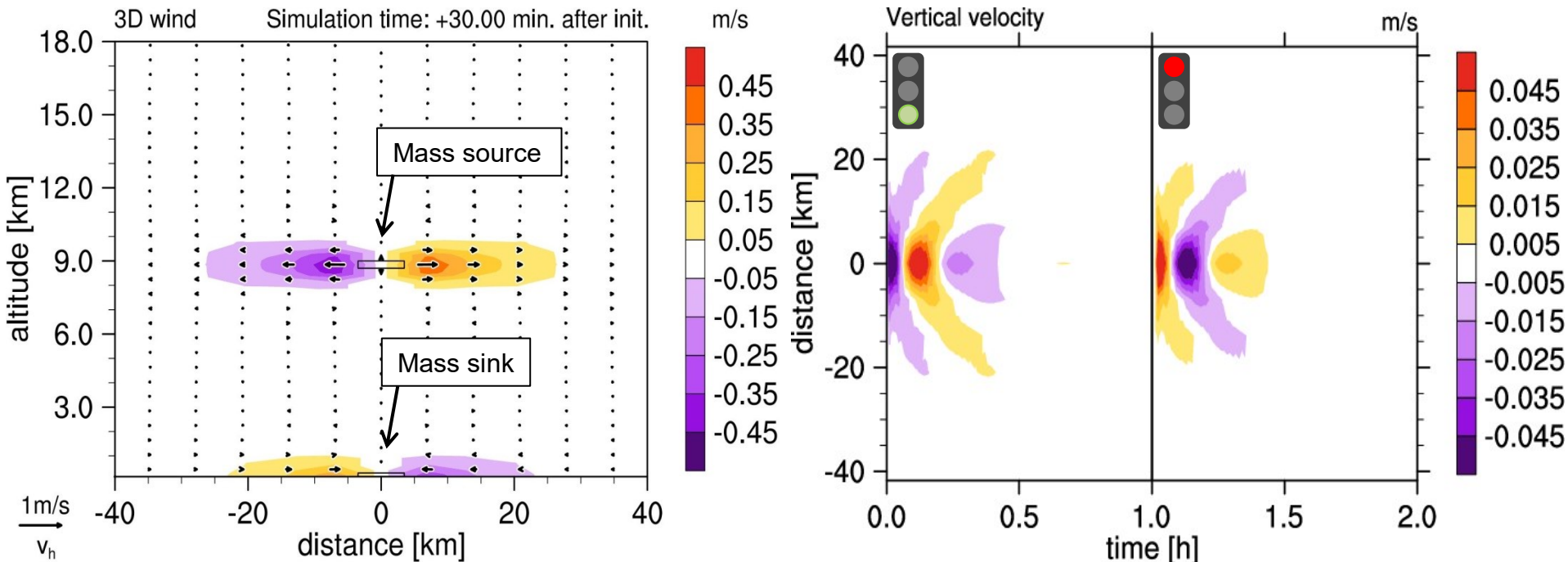
Specific ICON Setup

Triangular grid with
 $\Delta l_e = 10.5 \text{ km}$ ($A_{\text{ICON}} \cong A_{\text{COS}}$)

Mass Lifting Experiment

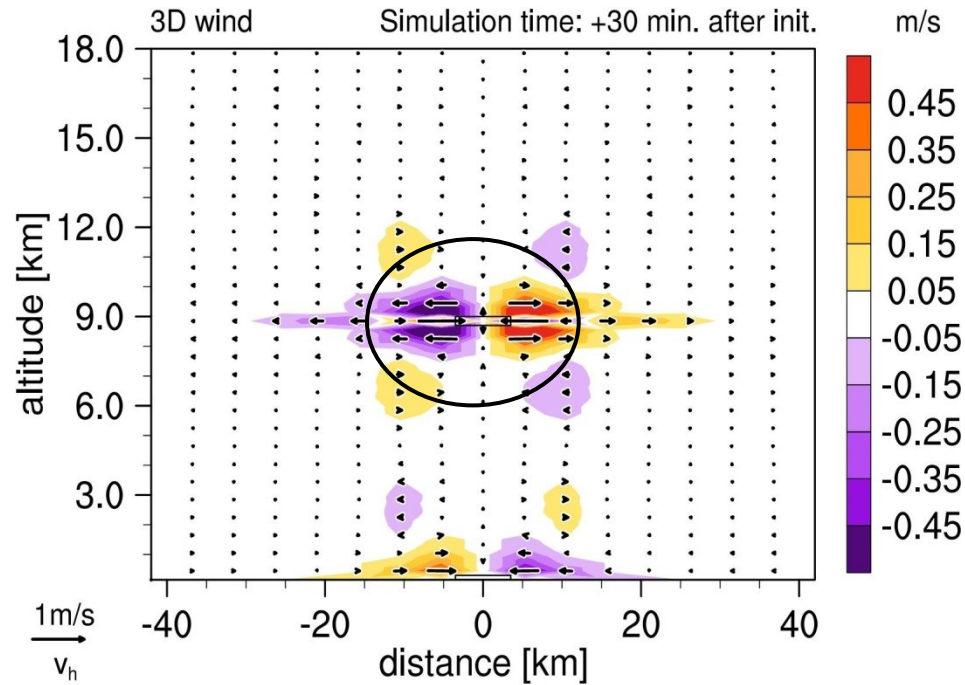
Results of COSMO simulation (v5.1., reference):

Dynamical flow response and gravity wave emission



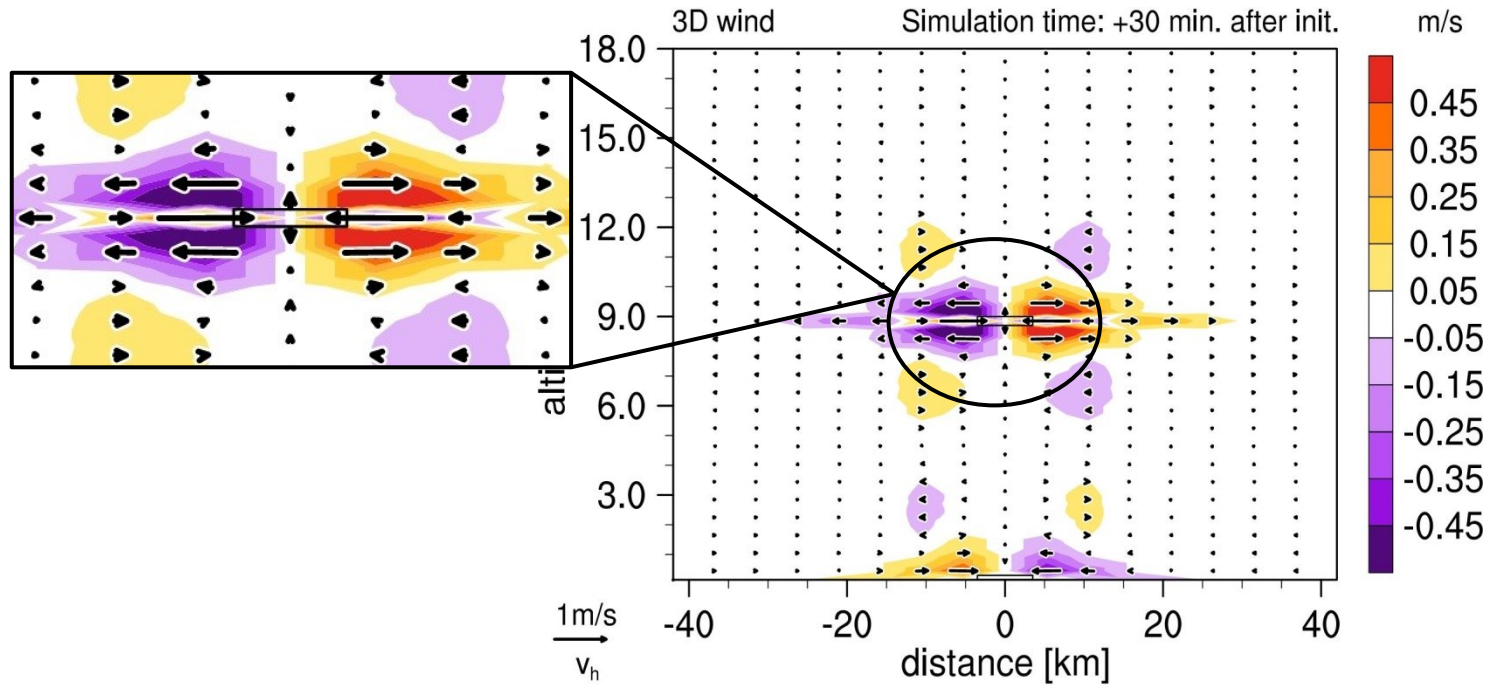
Mass Lifting Experiment

Results of an ad-hoc implementation in ICON:



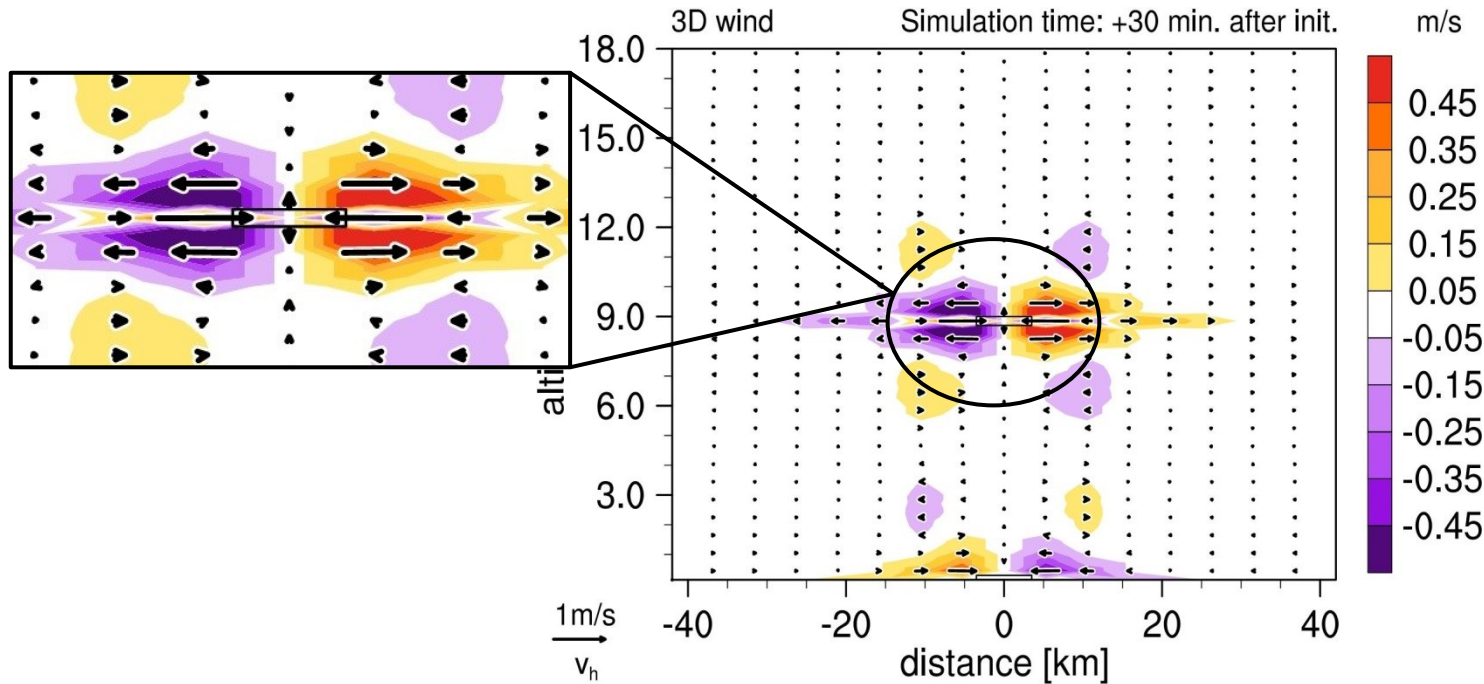
Mass Lifting Experiment

Results of an ad-hoc implementation in ICON:



Mass Lifting Experiment

Results of an ad-hoc implementation in ICON:



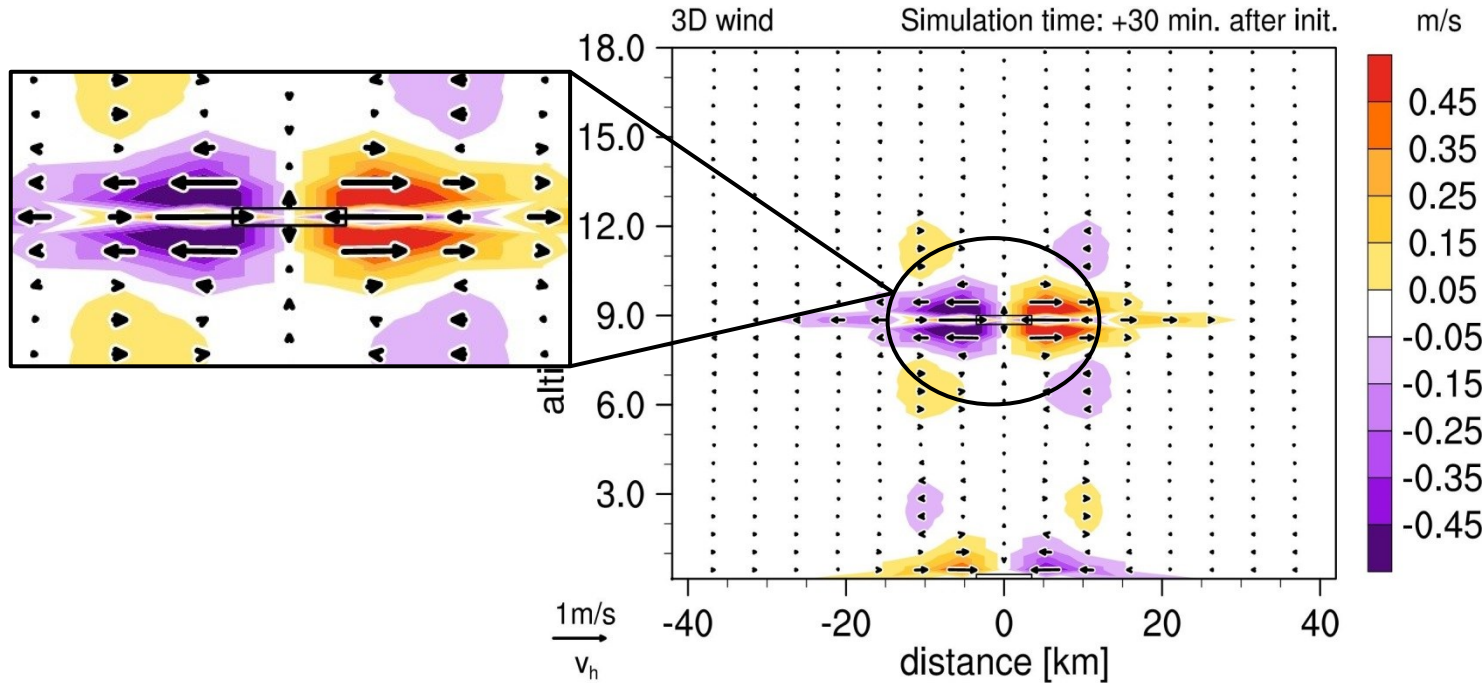
- Distorted dynamical response due to **anisotropic 4th order divergence damping**

$$\frac{\partial v_n}{\partial t} + \text{adv}(v_n) = -c_{pd} \theta_v \frac{\partial \pi}{\partial n} + F_s(v_n) + F_d(\mathbf{v})$$

$$\text{with } F_d(\mathbf{v}) = -f_d \bar{A}_c^2 \nabla_n \left(\tilde{\nabla} \cdot \left[\nabla_n \left(D_h + \frac{\partial w}{\partial z} \right) \right] \right)$$

Mass Lifting Experiment

Results of an ad-hoc implementation in ICON:



- Distorted dynamical response due to **anisotropic 4th order divergence damping**

$$\frac{\partial v_n}{\partial t} + \text{adv}(v_n) = -c_{pd} \theta_v \frac{\partial \pi}{\partial n} + F_s(v_n) + F_d(\mathbf{v})$$

with $F_d(\mathbf{v}) = -f_d \bar{A}_c^2 \nabla_n \left(\tilde{\nabla} \cdot \left[\nabla_n \left(D_h + \frac{\partial w}{\partial z} \right) \right] \right)$

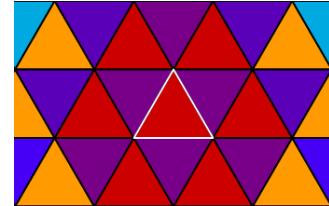
Vertical divergence affects v_n , but w is unaffected



So, what is the task of the divergence damping in ICON?

The Checkerboard Problem

- Major obstacle during development of ICON: Divergence polluted with checkerboard noise



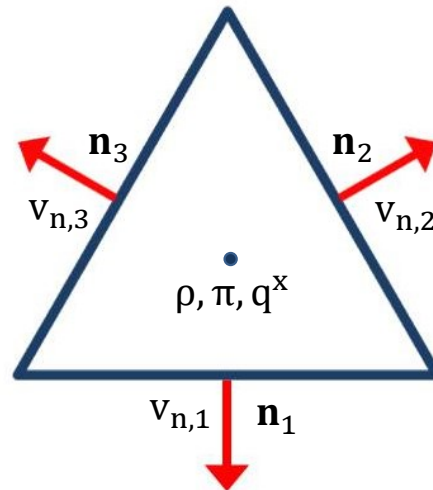
- Inherent property of the triangular grid (*Gassmann, 2011*):

- Vector components in trivariate coordinate system are linearly dependent

$$\tilde{v}_{n,1} + \tilde{v}_{n,2} + \tilde{v}_{n,3} = 0$$

- Any violation of the constraint gives rise to checkerboard noise

- Numerical filter (divergence damping, hyper-diffusion etc.) is indispensable !!!



Mitigating the Checkerboard Problem

Known approaches:

- **4th order divergence damping acting on 3D divergence** (operational, see *Zaengl et al. (2015)*)
- **Hyper-diffusion** (i.e. as in *Wan et al. (2013)*; different discretizations possible)



Strong grid imprinting



New approach:

→ Combination of divergence damping techniques (**CDD**)

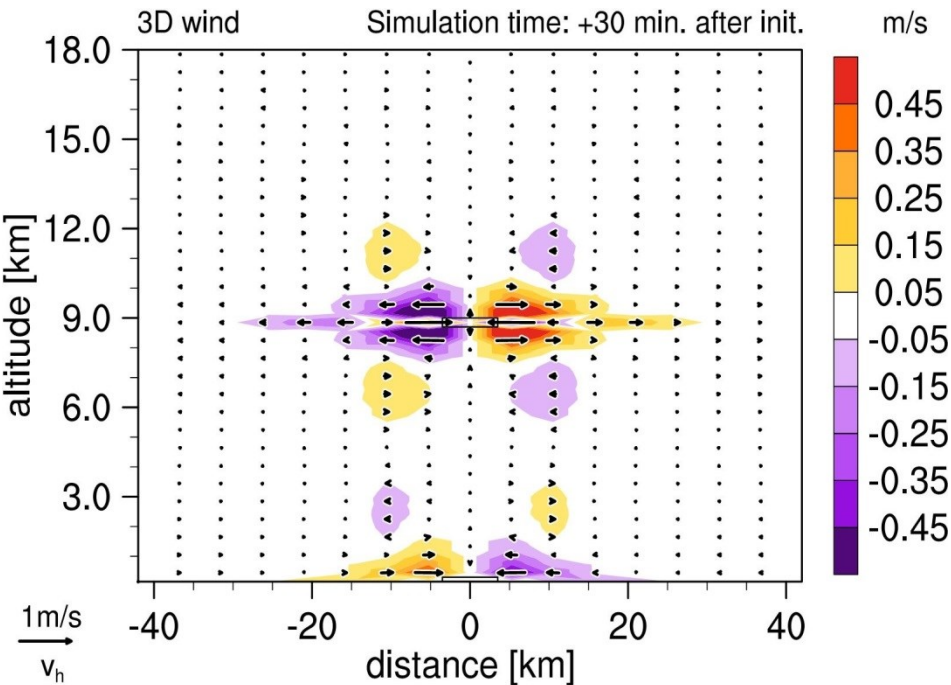
- **4th order divergence damping acting on 2D divergence**
 - ✓ Compatible with HYMACS
 - ✓ Very efficient noise filter
 - ✗ Damping of gravity waves
- **Isotropic 2nd order divergence damping**
 - ✓ Compatible with HYMACS
 - ✓ No degeneration of gravity waves
 - ✗ Less efficient noise filter

Mass Lifting Experiment

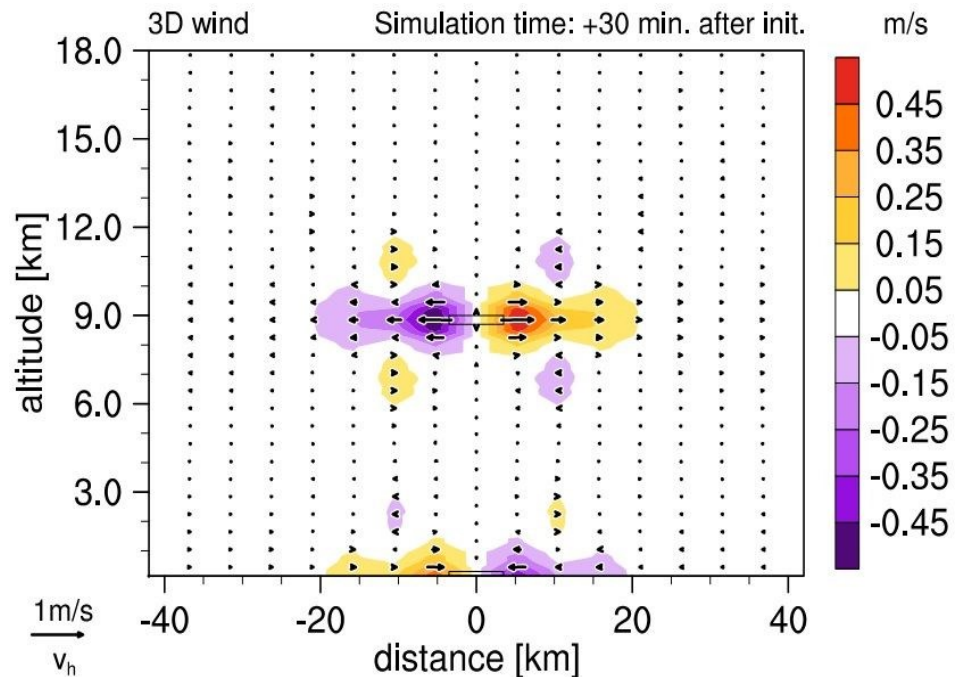
Results with combined divergence damping in dynamical core:

Dynamical flow response

Conventional divergence damping



Combined divergence damping

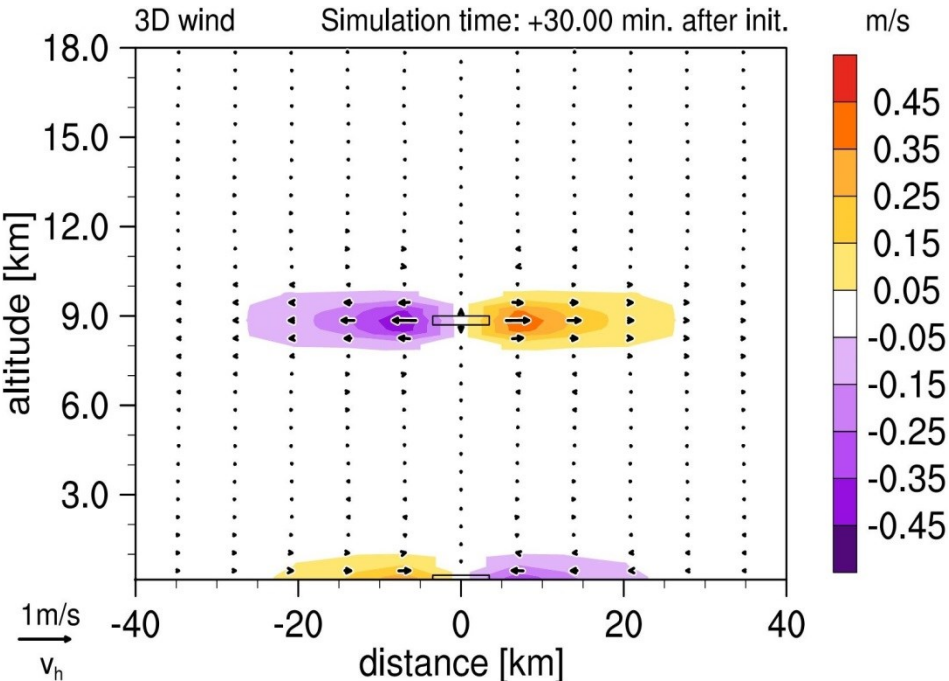


Mass Lifting Experiment

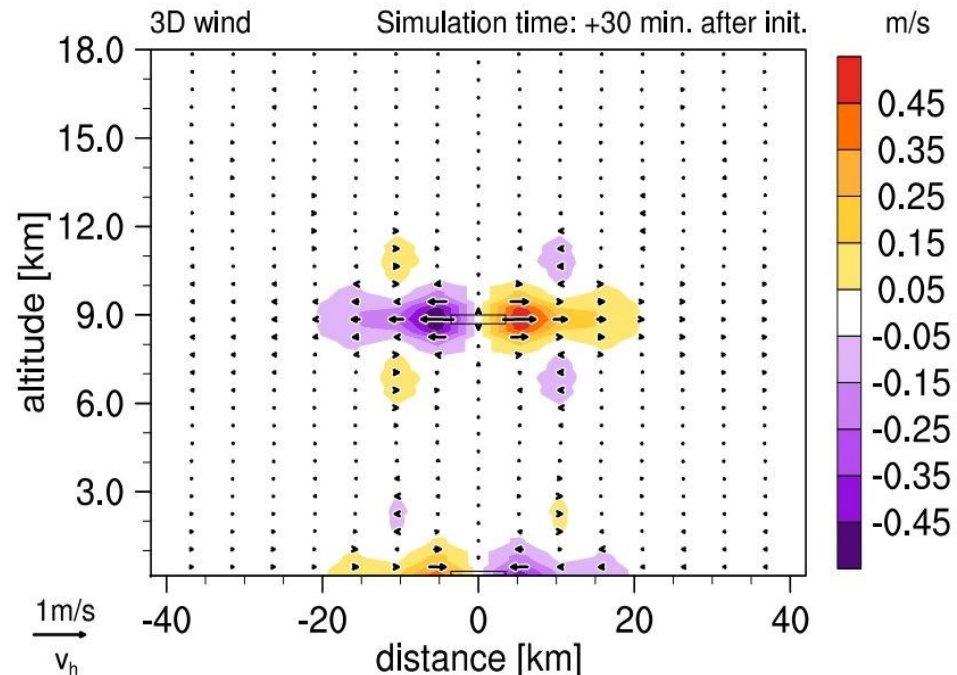
Results with combined divergence damping in dynamical core:

Dynamical flow response

COSMO (reference)



Combined divergence damping

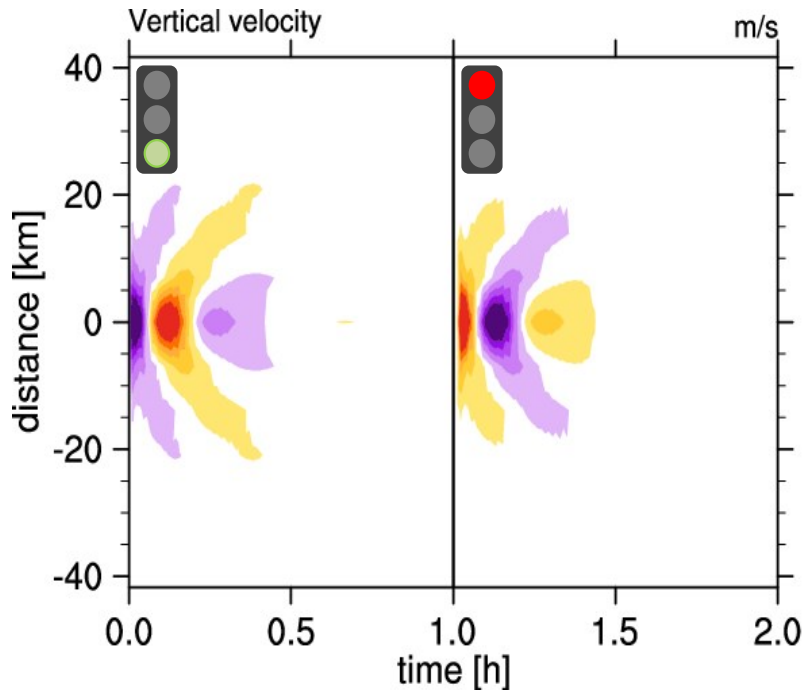


Mass Lifting Experiment

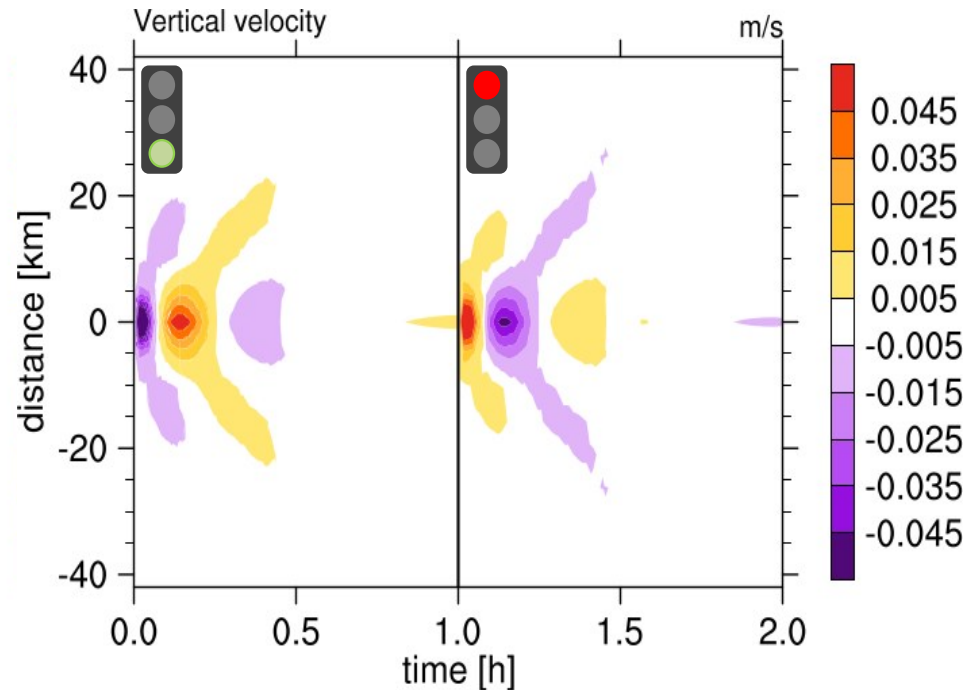
Results with combined divergence damping in dynamical core:

Gravity wave emission

COSMO (reference)



Combined divergence damping

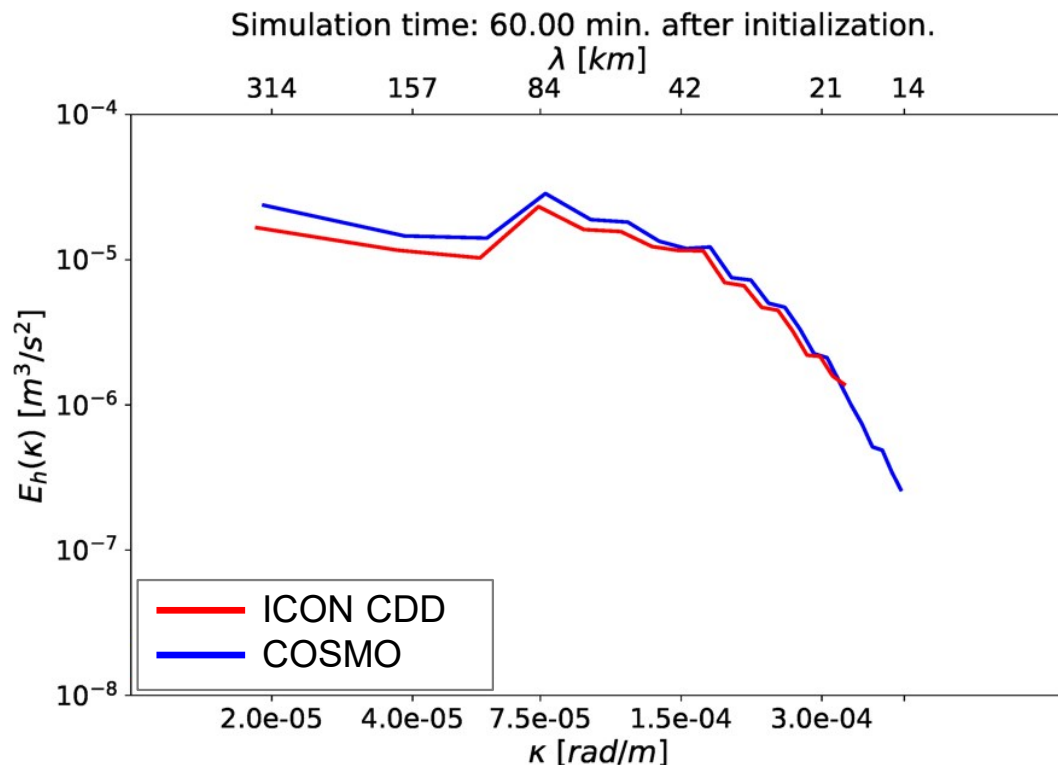


Mass Lifting Experiment

Results with combined divergence damping in dynamical core:

Quantifying Checkerboard-Noise in energy spectra

→ interpolation of horizontal wind onto regular grid ($\Delta x = 0.87\Delta l_e$ following *Dipankar et al. (2015)*) in ICON

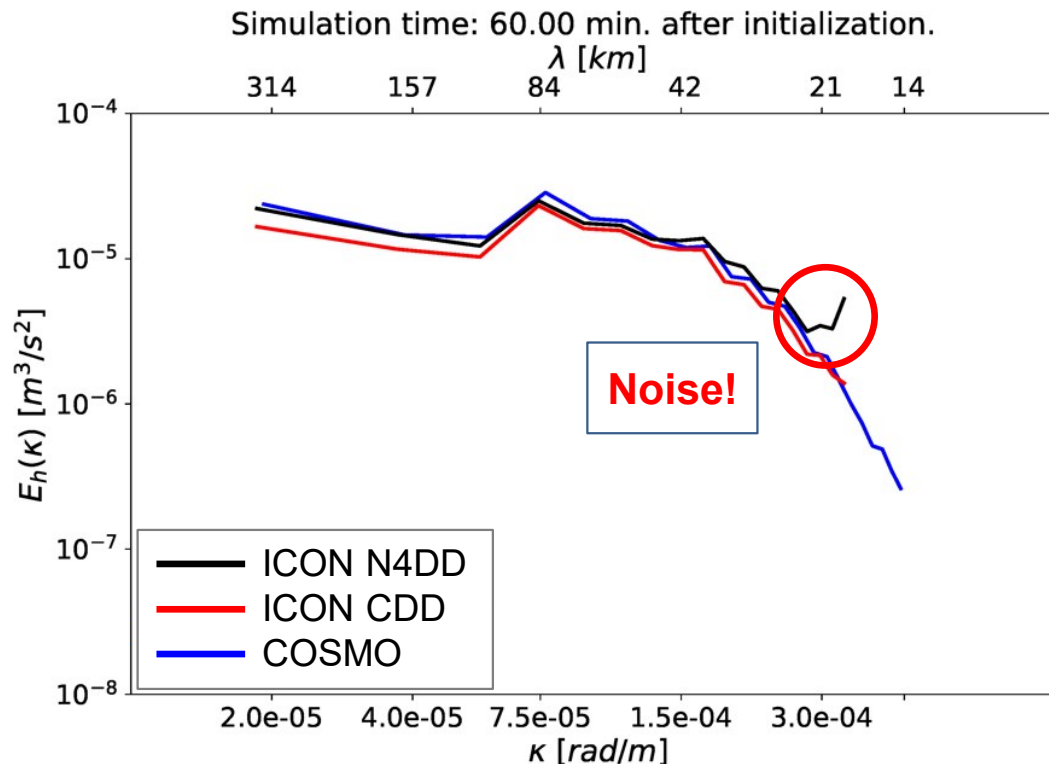


Mass Lifting Experiment

Results with combined divergence damping in dynamical core:

Quantifying Checkerboard-Noise in energy spectra

→ interpolation of horizontal wind onto regular grid ($\Delta x = 0.87\Delta l_e$ following *Dipankar et al. (2015)*) in ICON

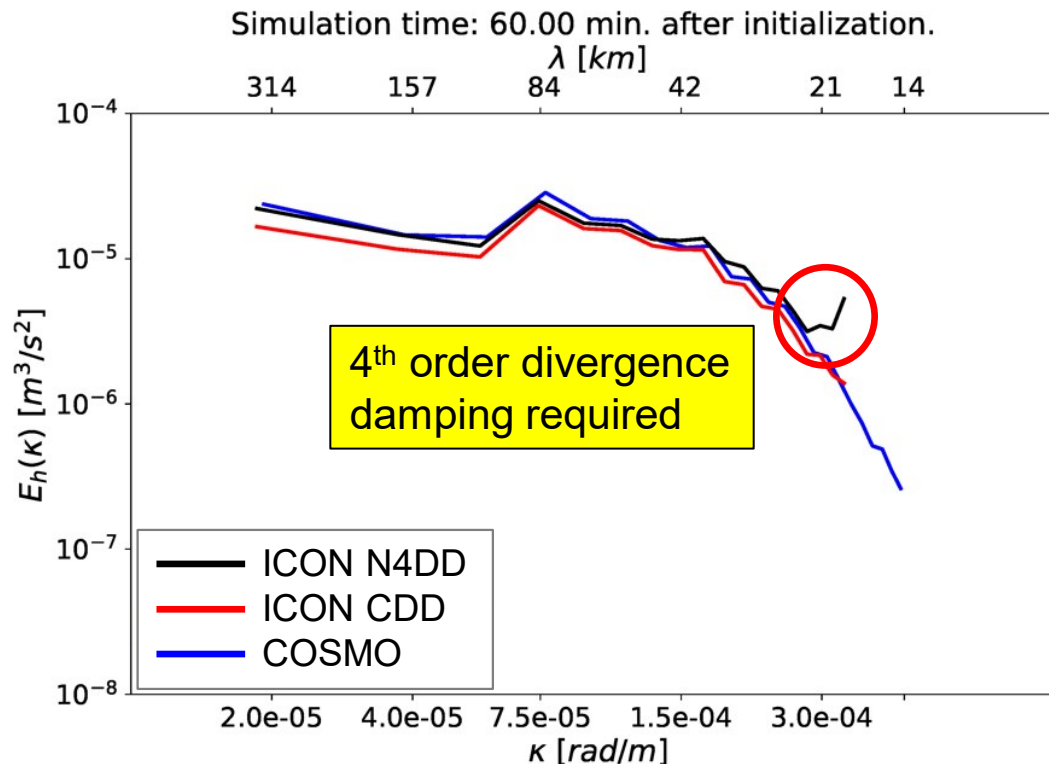


Mass Lifting Experiment

Results with combined divergence damping in dynamical core:

Quantifying Checkerboard-Noise in energy spectra

→ interpolation of horizontal wind onto regular grid ($\Delta x = 0.87\Delta l_e$ following *Dipankar et al. (2015)*) in ICON



Conclusion and Outlook

HYMACS in ICON is not trivial...

- no conventional physics-dynamics coupling
- inherent checkerboard problem in divergence of the triangular grid
 - ⚠ HYMACS forces divergent/convergent wind pattern at smallest model scale
 - ⚠ Conventional numerical filter inappropriate

Implementation of a combined divergence damping

- ✓ Compatible with HYMACS
- ✓ Effective reduction of checkerboard noise
- ✓ Comparable performance in Jabolonowski-Williamson test cases

Further steps

- Idealized tests with moisture (activated cloud model)
- Real case tests in ICON-LAM

HYMACS in ICON

First idealized tests and adaptations of the dynamical core to subgrid-scale mass fluxes

Michael Langguth, Volker Kuell and Andreas Bott



Sturmjäger NRW

ICCARUS 2019
DWD, Offenbach, 18th-20th March 2019

Offenbach, 2019/03/18

Literature

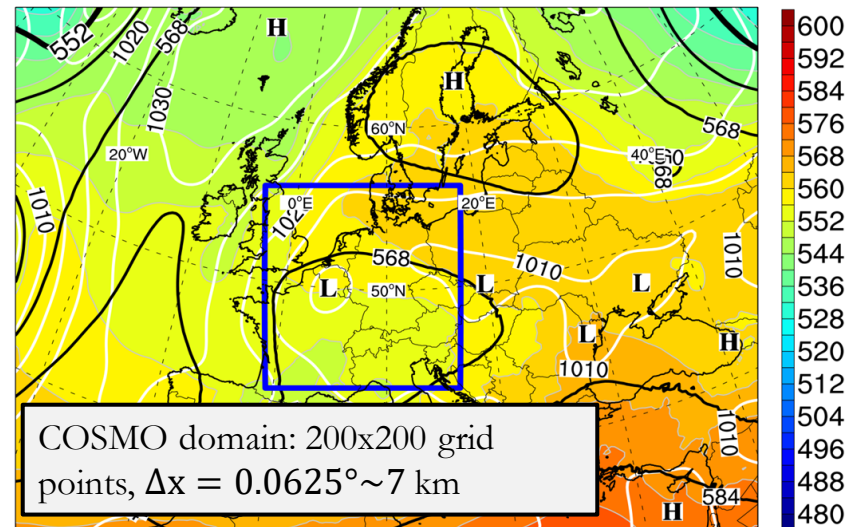
- Dipankar, A. et al. (2015). Large eddy simulation using the general circulation model ICON. *Journal of Advances in Modeling Earth Systems*, **7**, 963-986
- Gassmann, A. (2011). Inspection of hexagonal and triangular C-grid discretizations of the shallow water equations. *Journal of Computational Physics*, **230**, 2706-2721
- Kuell, V., Gassmann A., Bott, A. (2007). Towards a new hybrid cumulus parametrization scheme for use in non-hydrostatic weather prediction models. *Quarterly Journal of the Royal Society*, **133**, 479-490
- Kuell, V. and Bott, A. (2009). Application of the hybrid convection parametrization scheme HYMACS to different meteorological situations. *Atmospheric Research*, **94**, 743-753
- Kuell, V. and Bott, A. (2011). Simulation of non-local effects of convection with the hybrid mass flux convection scheme HYMACS. *Meteorologische Zeitschrift*, **20**, 227-241
- Ong, H., Wu, C. et al. (2017). Effects of artificial local compensation of convective mass flux in the cumulus parameterization. *Journal of Advances in Modeling Earth Systems*, **94**, 1811-1827
- Uebel, M. and Bott, A. (2015). Mesoscale air transport at a midlatitude squall line in Europe- a numerical analysis. *Quarterly Journal of the Royal Meteorological Society*, **141**, 3297-3311
- Wan, H. et al. (2013). The ICON-1.2 hydrostatic atmospheric dynamical core on triangular grids, Part I: formulation and performance of the baseline version. *Geoscientific Model Development*, **6**, 735-763
- Zaengl, G. et al. (2015). The ICON modelling framework of DWD and MPI-M: Description of the non-hydrostatic dynamical core. *Quarterly Journal of the Royal Meteorological Society*, **141**, 563-579

Special thanks go to **Daniel Reinert** and **Günther Zängl** for many helpful advices and valuable discussions.

Motivation

- Virtues of introducing net mass transfer in simulating deep convection:
 - Theoretically: idealized experiments of convective systems (*Shutts and Gray, 1994; Gray et al., 1998; Gray, 1999; Chagnon and Bannon, 2006; Kuell et al., 2007* etc.)
 - Practical applications: HYMACS in COSMO
- Case study with COSMO (v5.01) during a persistent high-over-low weather situation over Central Europe in June 2016:
 - Seven 24h-simulations with different CPS: HYMACS (HYM) and Tiedtke (Tie)
 - Verification against RADOLAN observations

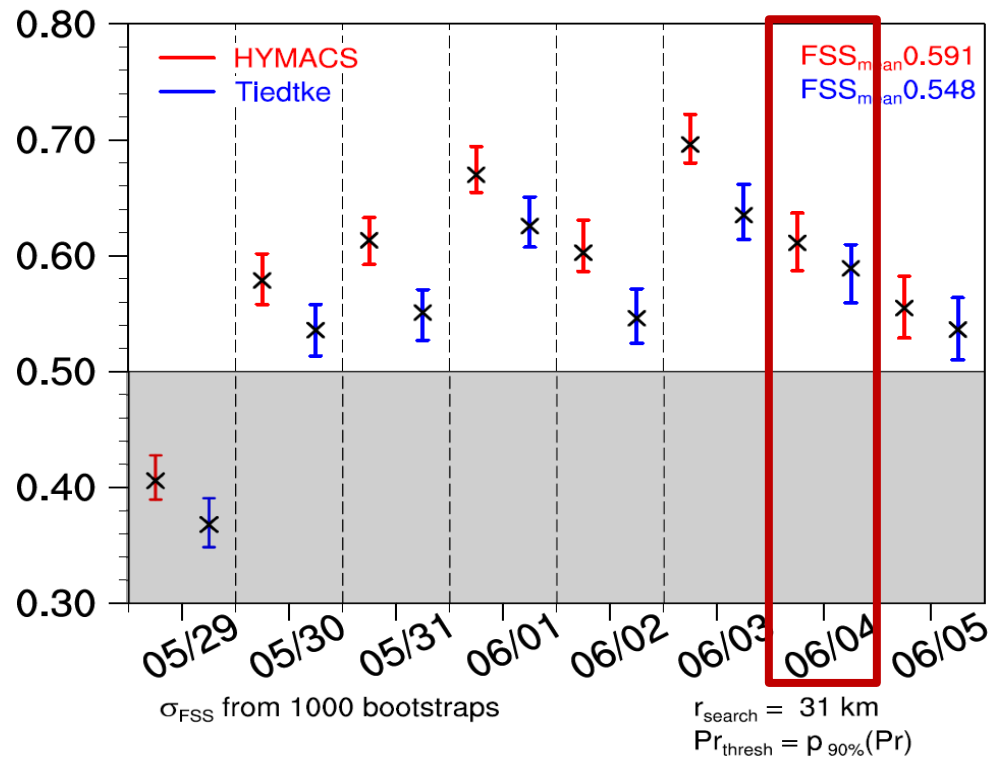
Rel. Topography, 500 hPa Geopotential, PMSL



Motivation

Spatial verification:

(Bias-corrected) Fractional Skill Score-analysis:

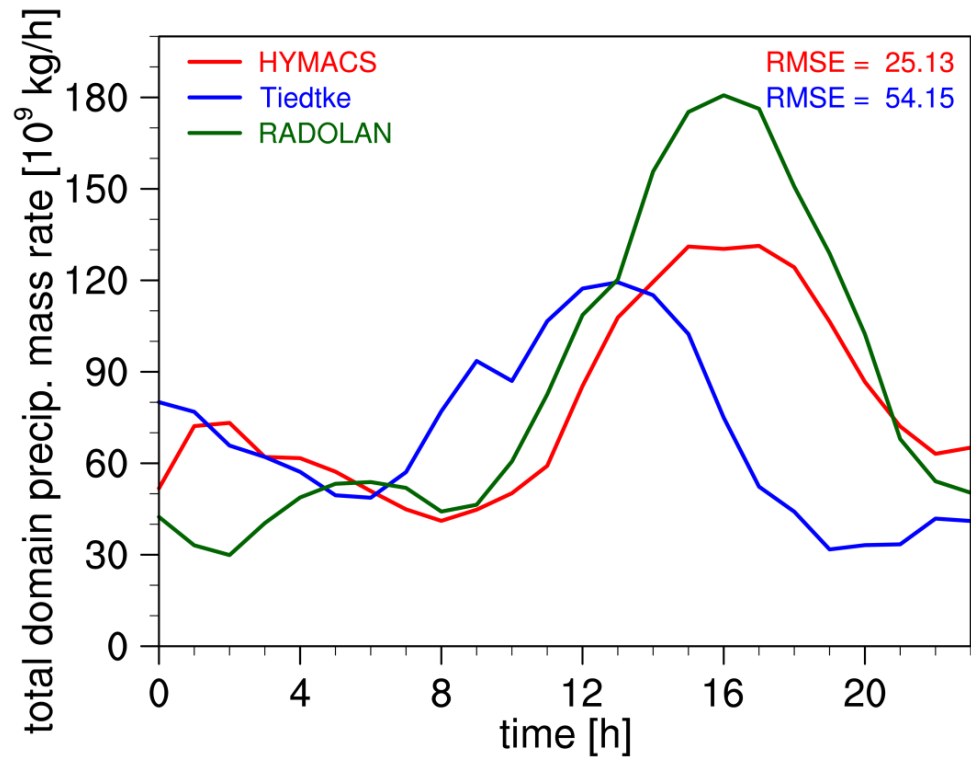


+ Better simulation of precipitation patterns with HYMACS

Motivation

Diurnal cycle:

Area-integrated precipitation rates:

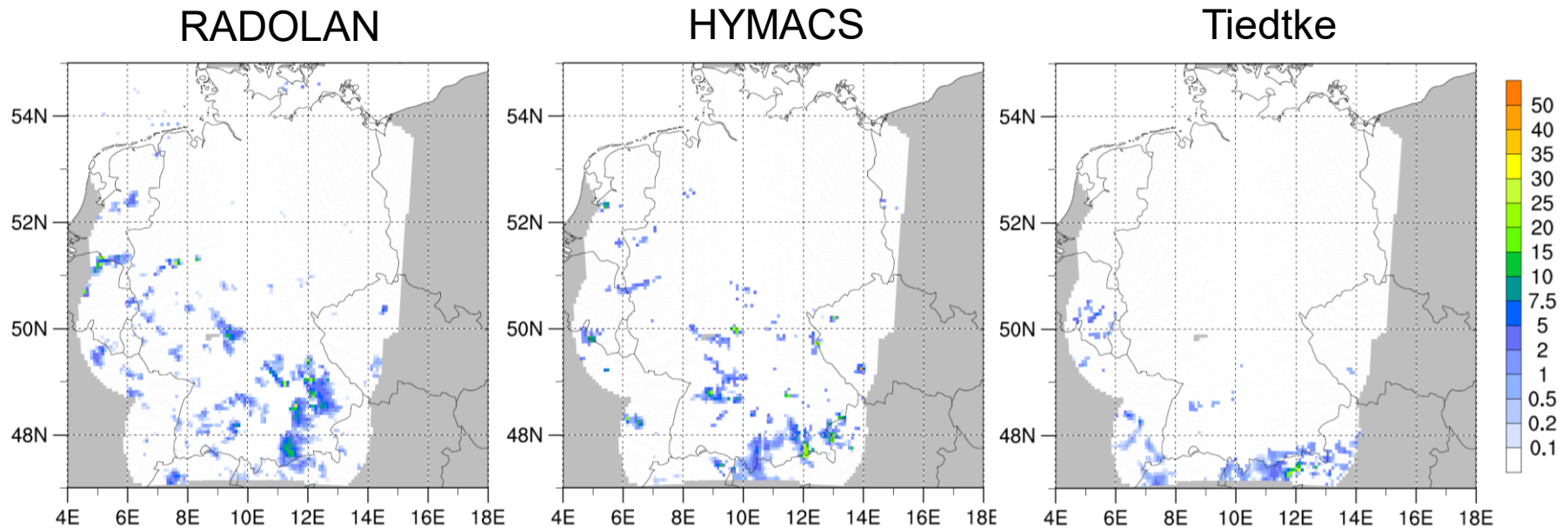


+ Better representation of the diurnal cycle with HYMACS

Motivation

Diurnal cycle:

Precipitation rates on 4th June 2016 20 UTC:



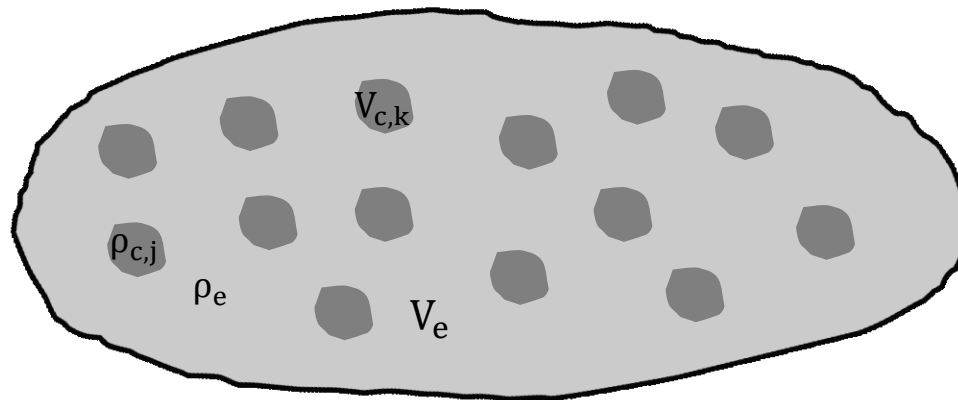
+ Better representation of the diurnal cycle with HYMACS

HYMACS - Theoretical Background

- Arbitrary volume consisting of environmental and convective part with partial densities ρ_e and ρ_c
- Momentum of conv. part $\tilde{\mathbf{v}}_c$ as superposition of environmental \mathbf{v}_e and convective \mathbf{v}_c
- Balance equation (no internal sources):

$$\begin{aligned} \frac{D\rho}{Dt} = 0 &= \frac{\partial\rho}{\partial t} + \nabla \cdot (\rho\mathbf{v}_e + \rho_c\mathbf{v}_c) \\ &= \frac{\partial\rho}{\partial t} + \nabla \cdot (\rho\mathbf{v}_e) + \nabla \cdot \mathbf{J}_c \end{aligned}$$

- Dominance



$$+ \frac{\partial M_d}{\partial z}$$

$$V = V_e + V_c = V_e + \sum_i^n V_{c,i}$$

Barycentric momentum:

$$\rho\mathbf{v} = \rho_e\mathbf{v}_e + \rho_c\tilde{\mathbf{v}}_c$$

Physics-dynamics coupling

- Convective tendency of any scalar ψ considering mass transfer

$$\left. \frac{\partial \psi}{\partial t} \right|_{\text{conv}} = \left(\frac{\rho(t^n)}{\rho^*} - 1 \right) \frac{\psi(t^n)}{\Delta t} - \frac{1}{A \Delta z \rho^*} (\varepsilon_{u,d} \psi - \delta_{u,d} \psi_{u,d})$$

$$\text{with } \rho^* = \rho(t^n) + \Delta t \left. \frac{\partial \rho}{\partial t} \right|_{\text{conv}}$$

- Update of density ρ and Exner pressure π through convective tendencies in the dynamical core
- π -tendency derived from 1st law of thermodynamics:

$$\left. \frac{\partial \pi}{\partial t} \right|_{\text{conv}} = \frac{R_d}{c_{vd}} \frac{\pi}{\rho} \left. \frac{\partial \rho}{\partial t} \right|_{\text{conv}} + \frac{1}{\theta_v} \frac{R_d (1 + \alpha)}{c_{vd} c_{pd}} \left. \frac{\partial h}{\partial t} \right|_{\text{conv}} + \frac{R_d \pi}{c_{vd} (1 + \alpha)} \left. \frac{\partial \alpha}{\partial t} \right|_{\text{conv}}$$

$$\text{with } \alpha = \left(\frac{R_d}{R_v} - 1 \right) q^v - q^l - q^f$$

- Update of moisture species q^x and momentum v_n at physical time step (conventional approach)

Similarity of diffusion and divergence damping

- Former diffusion operator based on identity of vector laplacian (Wan et al., 2013)

$$\begin{aligned}\nabla^2 \mathbf{v} &= \nabla(\nabla \cdot \mathbf{v}) - \nabla \times (\nabla \times \mathbf{v}) \\ \Rightarrow (\nabla_d^2 \mathbf{v})_e \cdot \mathbf{N}_e &= \nabla_n(D_h) - \nabla_t \zeta\end{aligned}$$

- Properties of the fourth-order hyper laplacian $(\nabla_d^4 \mathbf{v})_e \cdot \mathbf{N}_e = \nabla_d^2(\nabla_d^2 \mathbf{v})$

Advantage	Disadvantage
✓ Effective noise removal	✗ High diffusivity required for effective noise removal
	✗ Numerical errors near pentagon points (→ distorted triangles)

- First term of hyper laplacian operator **corresponds** to fourth order divergence damping term (involving D_h)



Fourth order divergence damping may be tuned to remove checkerboard pattern **without** excessive diffusivity

Isotropic 2nd order divergence damping

- implicit numerical solution process for prognostic vertical wind
→ standard algorithm for three-band matrix (Thomas algorithm)
- Damping term applied in corrector step of two-timelevel integration scheme

$$AD = f_{d,2o} A_c \left(\beta_1 \left(\frac{\partial D_h}{\partial z} + \frac{\partial}{\partial z} \left(\frac{\partial w}{\partial z} \right) \right)^{n+1} + \beta_2 \left(\frac{\partial D_h}{\partial z} + \frac{\partial}{\partial z} \left(\frac{\partial w}{\partial z} \right) \right)^{n+1*} \right)$$

with $\beta_1 = 1 - \beta_2$: Crank–Nicholsen parameter

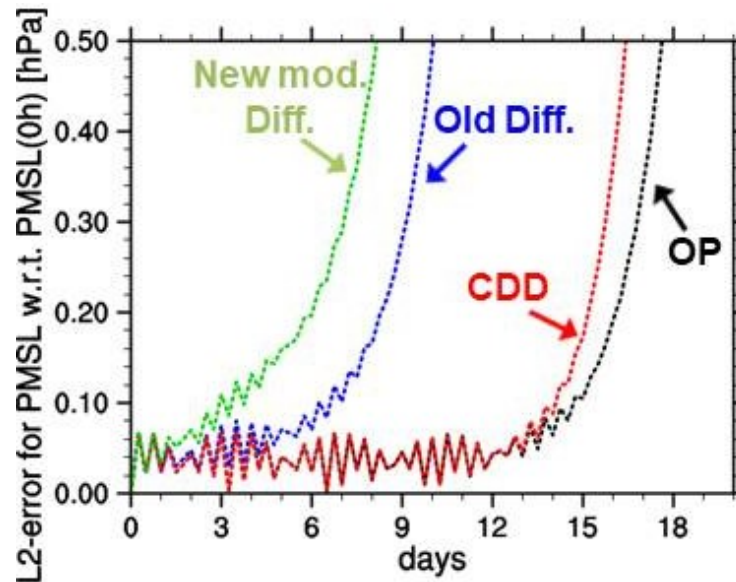
and $n+1$: new timelevel, $n+1^*$: intermediate timelevel

- Less scale-selective than 4th order divergence damping
- Averaging of D_h for *pure* 2nd order divergence damping → reduce noise, but not fully isotropic



Jabolonowski-Williamson test cases

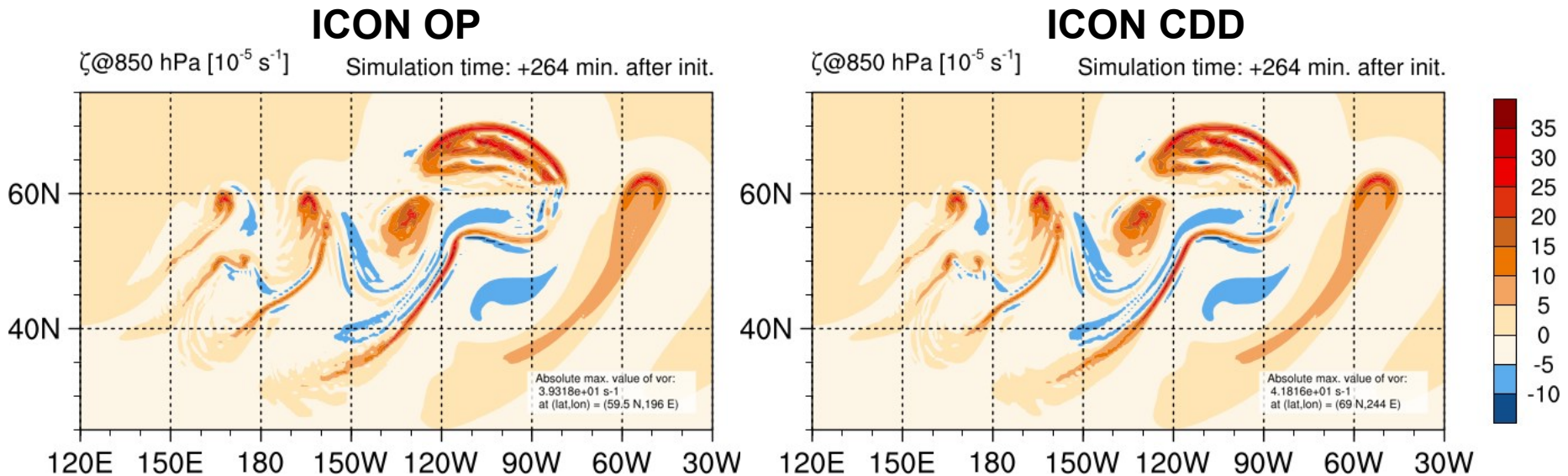
- Standard test for dyn. cores of global models (*Jabolonowski and Williamson, 2006*)
- *Steady state* configuration:
 - Zonally symmetric, strong baroclinic atmosphere
 - No perturbation imposed, i.e. hydrostatic and geostrophic balance
- Grid imprinting due to numerical discretization errors become visible → baroclinic wave development
- L2 error of surface pressure > 0.5 hPa → initial state broken



Baroclinic wave test case

➤ Baroclinic wave configuration:

- Initialization with zonal wind perturbation
→ triggers (explosive) baroclinic wave train after 7 days



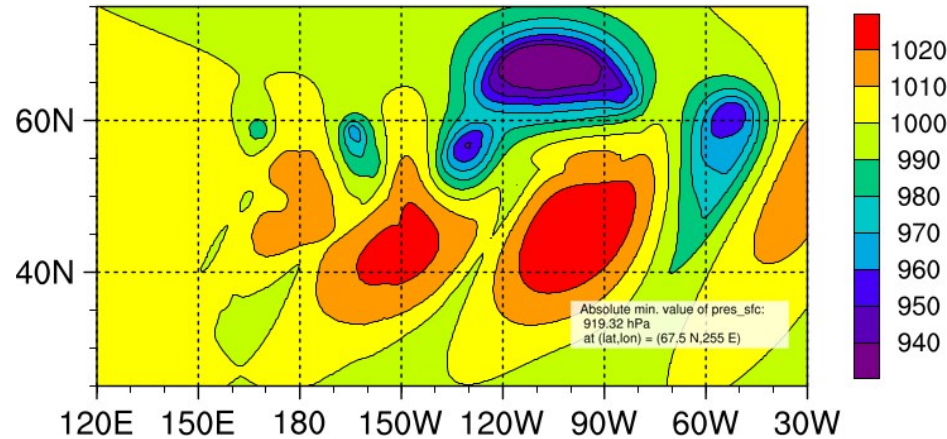
Baroclinic wave test case

➤ Baroclinic wave configuration:

- Initialization with zonal wind perturbation
→ triggers (explosive) baroclinic wave train after 7 days

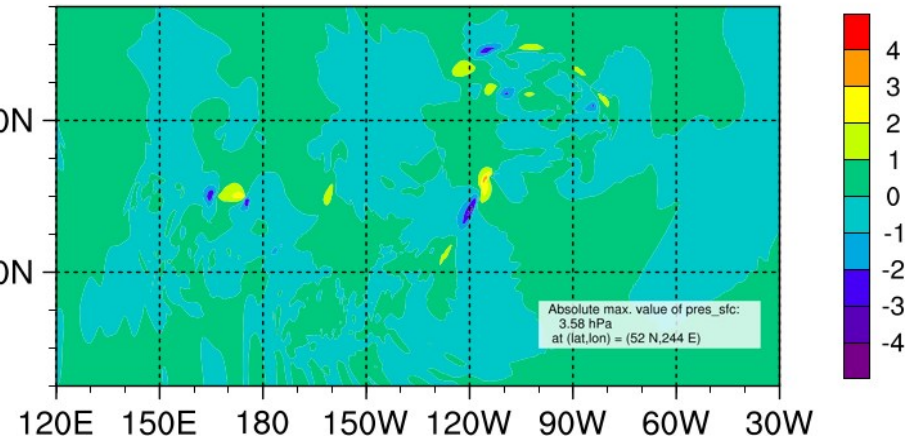
ICON CDD

surface pressure Simulation time: +264 h after init.



ICON CDD – ICON OP

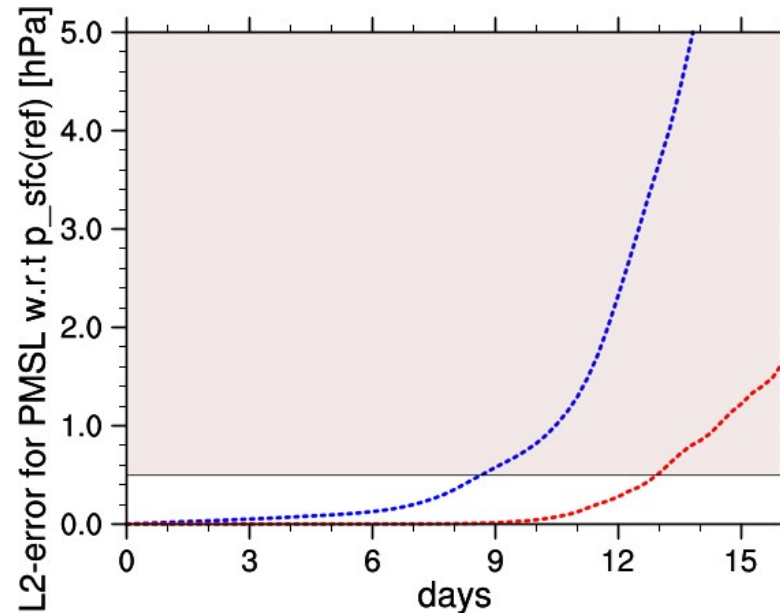
diff. in surface pressure Simulation time: +264 h after init.



Baroclinic wave test case

➤ *Baroclinic wave* configuration:

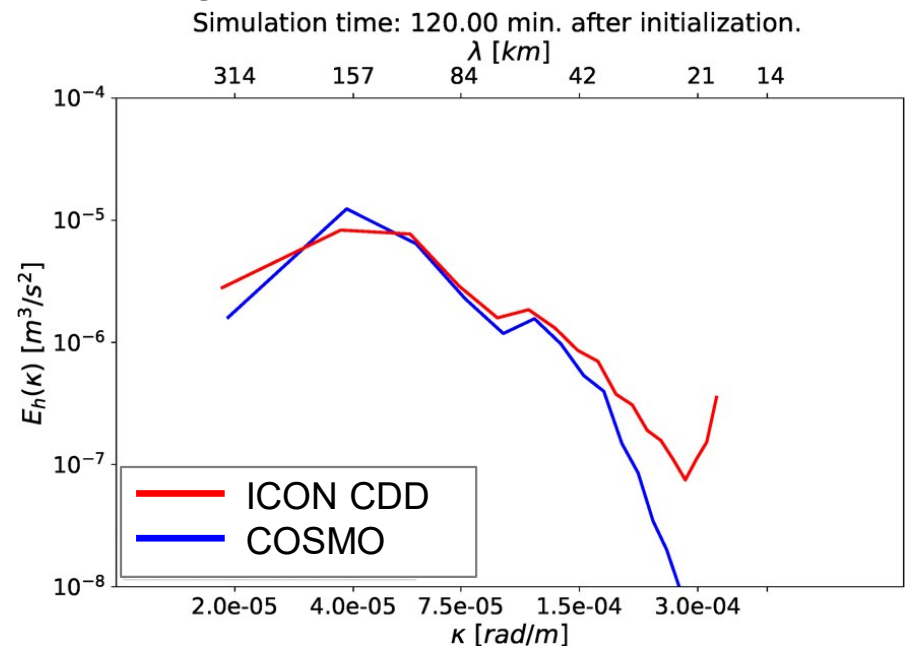
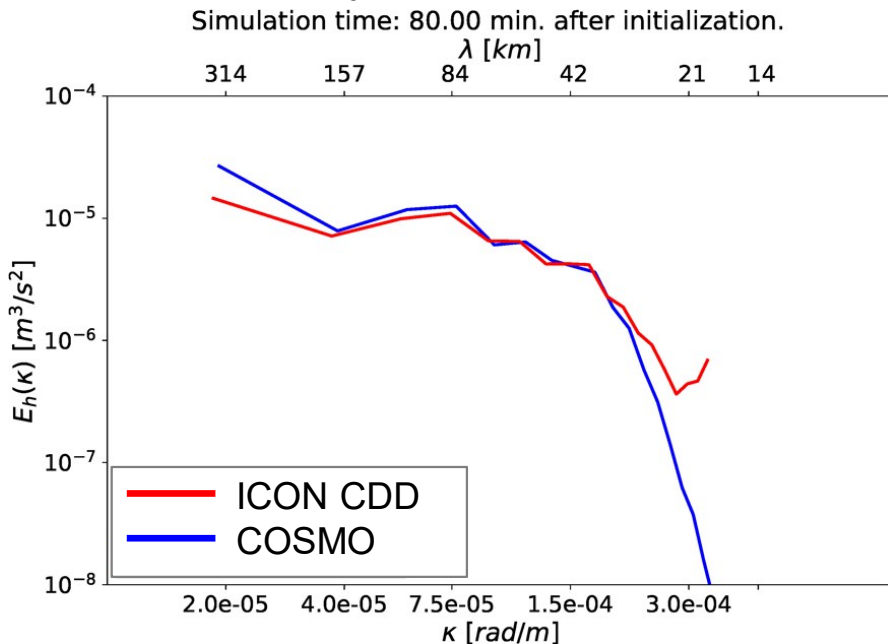
- Initialization with zonal wind perturbation
→ triggers (explosive) baroclinic wave train after 7 days



- ✓ Baroclinic wave train practically indistinguishable until simulation day 13

Noise in the dissipation phase

- In principle, dynamical response ok after switching off mass transfer, but...



- Slower dissipation at shortest wave spectrum $\lambda \sim 2\Delta x$
- Quicker dissipation at $\lambda \sim (3 - 5)\Delta x$ due to 2nd order divergence damping

Further testing required with focus on real case studies